Talanta 130 (2014) 20–25

Contents lists available at ScienceDirect

Talanta

journal homepage: www.elsevier.com/locate/talanta

Ultra sensitive label free surface enhanced Raman spectroscopy method for the detection of biomolecules

Juanita Hughes [a,b], Emad L. Izake [a,b,*], William B. Lott [a,b], Godwin A. Ayoko [a,b], Martin Sillence [a,b]

[a] Nanotechnology and Molecular Sciences Discipline, Faculty of Science and Engineering, Queensland University of Technology, 2 George St., Brisbane 4001, QLD, Australia
[b] Discipline of Biosciences, Faculty of Science and Engineering, Queensland University of Technology, 2 George St., Brisbane 4001, QLD, Australia

ARTICLE INFO

Article history:
Received 2 May 2014
Received in revised form
9 June 2014
Accepted 10 June 2014
Available online 30 June 2014

Keywords:
Ultra trace analysis
Label-free SERS
Nanosensor
Erythropoietin
Caffeine

ABSTRACT

We present a proof of concept for a novel nanosensor for the detection of ultra-trace amounts of bio-active molecules in complex matrices. The nanosensor is comprised of gold nanoparticles with an ultra-thin silica shell and antibody surface attachment, which allows for the immobilization and direct detection of bio-active molecules by surface enhanced Raman spectroscopy (SERS) without requiring a Raman label. The ultra-thin passive layer (~1.3 nm thickness) prevents competing molecules from binding non-selectively to the gold surface without compromising the signal enhancement. The antibodies attached on the surface of the nanoparticles selectively bind to the target molecule with high affinity. The interaction between the nanosensor and the target analyte result in conformational rearrangements of the antibody binding sites, leading to significant changes in the surface enhanced Raman spectra of the nanoparticles when compared to the spectra of the un-reacted nanoparticles. Nanosensors of this design targeting the bio-active compounds erythropoietin and caffeine were able to detect ultra-trace amounts the analyte to the lower quantification limits of 3.5×10^{-13} M and 1×10^{-9} M, respectively.

1. Introduction

Raman spectroscopy is a rapid, non-destructive vibrational spectroscopy that relies on inelastic light scattering by analyte molecules and, therefore, provides a unique spectroscopic signature that potentially identifies the species. Sharp bands of good resolution, which make the technique ideal for distinguishing between closely related molecules, are also characteristic of Raman spectroscopy [1–6].

Surface enhanced Raman spectroscopy (SERS) is a Raman spectroscopic technique that significantly amplifies the inherently weak Raman signal. The phenomenon responsible for SERS occurs at the surface of coinage metals (Au, Ag or Cu), and the principal electromagnetic enhancement mechanism depends upon the nano-scale roughness features of the metal surface. Thus, SERS can potentially be observed either on roughened bulk metal surfaces or on the surfaces of metal nanoparticles (NPs). When incident light interact with the nanoparticles, it may induces collective oscillations of the electrons on the surface of the nanoparticles. These oscillations result in a substantial electromagnetic field known as the Localised Surface Plasmon Resonance (LSPR) [3]. The LSPR decays exponentially with the distance from the NP surface, and is reduced to virtually zero at 10 nm [6]. When the analyte molecule is within the effective range (< 5 nm) [6] of the LSPR, a dipole moment is induced in the molecule. This leads to as large as a million fold Raman signal enhancement with a single isolated NP [5]. “Hotspots” are created when multiple NPs reside within each other's effective LSPR range (< 1 nm is optimal) [3] and exhibit an extraordinary Raman signal enhancement as large as 1×10^{14}, allowing sensitivity of up to single-molecule detection [6].

Due to its high sensitivity, SERS has the potential to detect many bio-active molecules that normally exist in ultra-trace amounts. For example, SERS has been reported to detect proteins in biological samples [7]. SERS-based methods for protein detection can be divided into two types: (1) label-free and (2) Raman dye-labelled. The label-free strategy traditionally relies on directly adsorbing proteins onto bare metallic substrates and acquiring the vibrational information about the proteins themselves [8–10,11,12]

* Corresponding author at: Nanotechnology and Molecular Sciences Discipline, Faculty of Science and Engineering, Queensland University of Technology, 2 George St., Brisbane 4001, QLD, Australia. Tel.: +61 7 3138 2501; fax: +61 7 3138 1804.
E-mail address: e.kiriakous@qut.edu.au (E.L. Izake).

http://dx.doi.org/10.1016/j.talanta.2014.06.012
0039-9140/

by SERS. Raman dye-labelled methods detect proteins indirectly by monitoring the SERS signal of a Raman label (reporter) that is attached to the metallic SERS substrate. Metal NPs that are functionalised with various Raman dyes (Cy3, Cy5, MBA, DSNB, RhB) have been reported to indirectly detect target proteins [8,13,14].

The SERS detection of molecular species that do not have strong affinity for the SERS substrate is problematic. This is particularly true in complex fluids containing multiple species, in which competing moieties with higher affinities than the desired analyte could potentially bind to the substrate to the exclusion of other species. In addition, the competitive binding of multiple species to the metallic surface of the SERS substrate usually leads to a complex SERS spectrum in which the extraneous signals obscure the fingerprint of the target analyte [15]. To prevent non-specific binding to the metallic surface and protect the Raman label from cross-reacting with interfering molecules, SERS substrates used in bioanalytics are frequently coated with a passive layer. This passive layer can be made of polymer or silica, and is usually >20 nm thick [16–19]. The thickness of this layer, however, compromises the Raman fingerprint of the target analyte, and only indirect measurement is available through the detection of the Raman fingerprint of the reporter.

In this study, we developed a novel label-free SERS nanosensor for ultra-trace detection and analysis of both large and small bioactive molecules. Incorporation of an antibody-functionalized thin silica coating eliminates the need to incorporate a Raman reporter, avoids the interfering spectrum from a Raman label, and allows the observation of molecular vibrational information directly from the target analyte.

2. Experimental

2.1. Chemicals and antibodies

Trisodium Citrate, Silver Nitrate, (3-aminopropyl)-trimethoxysilane (APTMS), Sodium Silicate, 3-(trihydroxysilyl)-propylmethylphosphonate (THPMP), Glutaraldehyde and Ethylamine were purchased from Sigma Aldrich. Gold (III) chloride and Caffeine standard were purchased from ProSciTech, Queensland, Australia.

Human Urinary Erythropoietin International Standard (HuEPO IS, 2nd International Reference Preparation) and recombinant Human Erythropoietin International Standard (rHuEPO IS, 3rd International Reference Preparation) were sourced from the National Institute for Biological Standards and Control, UK.

Mouse monoclonal anti-Caffeine antibody (ab15221) was purchased from Sapphire BioScience Pty. Ltd., New South Wales, Australia. Mouse monoclonal anti-Erythropoietin (EPO) antibody (3F6) was purchased from MAIIA Diagnostics, Uppsala, Sweden.

Caffeine-free diet Coca-Cola (Coca-Cola, Australia) and Devondale skim milk (Devondale—MG, Victoria, Australia) were obtained from a supermarket and used to assess the blocking efficiency of the ethylamine blocking agent and the nonspecific binding of the respective antibody-functionalised nanoparticles.

2.2. Synthesis and characterization of antibody-functionalized nanoparticles

The bare gold NPs were synthesised by a modified literature method [20]. Briefly, 88.8 μL $AuHCl_4$ (aq, 0.5 M), 29 μL distilled water, 17 μL $AgNO_3$ (aq, 0.1 wt%) and 2 mL trisodium citrate (aq, 1 wt%) were stirred at room temperature for 3 min, then added to 20 mL of distilled water (95 °C). The mixture was then stirred and refluxed for 5 min to develop the NP colloid. To coat the gold NPs with silica, 131.25 μL of 1 mM aqueous APTMS were added to the previous colloid and stirred at room temperature for 15 min. Eighty-four μL of aqueous sodium silicate (0.54% v/v, pH10) were then added, and the solution was stirred for a further 5 min at room temperature, before raising the temperature to 90 °C and stirring for 20 min [21]. The silica-coated NPs were isolated by centrifugation and washed with ethanol, air dried then resuspended in distilled water.

To introduce terminal amino groups to the silica surface, 1.68 mL of aqueous THPMP (5% v/v) were mixed with the NP solution and stirred at room temperature for 1 h. The THPMP-primed NP solution was then mixed with 8 mL of 1 mM aqueous APTMS (adjusted to pH 5 with acetic acid) and stirred for 30 min at 35 °C. Glutaraldehyde terminals were then attached to the modified silica surface by amide linkage where the NPs were resuspended in glutaraldehyde (10% v/v in PBS (pH 7.4)) and sonicated for 30 min. Following the glutaraldehyde attachment, the NPs were isolated by centrifugation and washed with PBS (pH 7.4), air dried then resuspended in distilled water. The washing procedure was repeated after each of the subsequent manufacturing steps.

To functionalise the NPs with the antibody, the NPs were resuspended in the appropriate antibody solution in PBS (pH 7.4) and incubated at 4 °C overnight to develop amide linkages between the glutaraldehyde terminals and the amine groups of the antibody. The glutaraldehyde terminals serve as linkers between the antibody and the silica shell. To block any remaining unreacted glutaraldehyde terminals, the antibody-functionalised NPs were resuspended in 1.5 mL of 0.7% (v/v in PBS) ethylamine and incubated at 4 °C for 30 min.

2.3. Instrumentation and spectroscopic measurements

The NPs were characterised by UV–visible spectroscopy [Cary 100 spectrophotometer (Agilent Technologies, USA)] and high resolution transmission electron microscopy (HrTEM) [JEOL JEM-2100F TEM (JEOL, USA)].

For the Raman spectroscopy measurements, 10 μL of the analyte (caffeine or EPO) solution were mixed with an equal volume of the relevant antibody-functionalised NP solution. The mixture was then allowed to stand for 10 min for caffeine and 30 min for EPO, respectively. The standing times had been optimised for each analyte to ensure complete binding between the analyte and the antibody (data not shown). The NP solutions were then deposited on microscope slides and allowed to air dry. Raman spectra were collected on the Renishaw in Via Raman Microscope using an excitation wavelength of 785 nm and 5% of maximum (450 mW) laser power. Spectra were collected using a 50× objective lens over a wavelength range from 350 cm^{-1} to 1700 cm^{-1} using 10 accumulations of 10 s exposure times each for a minimum of six independent measurements. To confirm the efficient blocking of the unreacted glutaraldehyde linker and the selectivity of the antibody-functionalised NPs towards the relevant target analyte, 30 μL of either caffeine-free Diet Coke™ or skim milk were added to equivalent volumes of antibody-functionalised NP colloids (anti-caffeine antibody and anti-EPO antibody, respectively). The mixtures were allowed to stand for the optimised binding time, and then the NPs were isolated from solution by centrifugation and washed with PBS buffer until no sign of discolouration and/or cloudiness was observed. The washed NPs were re-suspended in 20 μL of PBS buffer, deposited on a microscope slides, and screened by Raman spectroscopy. These data were compared to the spectra of the relevant un-reacted antibody-functionalized NPs.

3. Results and discussion

The plasmonic properties of the bare and silica-coated NPs were characterised by UV–visible spectroscopy. Both bare and

silica-coated NPs exhibited a characteristic absorption band at 527 nm. The average size of the silica-coated NPs determined by Hr-TEM measurements was 26 nm (Fig. 1A), while the thickness of the silica shell ranged from 0.5 nm to 3 nm with an average of ~1.3 nm (Fig. 1B). The silica coat acts as a passive shell to prevent non-specific binding to the gold NP surface. The passive shell was functionalised with antibodies attached to the surface via a glutaraldehyde linker molecule. This short linker allowed the antibody and the antibody-bound target analyte to reside in close proximity to the NP surface, within the effective LSPR range [6]. The SERS spectra of the bare gold nanoparticles and that of the nanoparticles after the attachment of the glutaraldehyde linker are shown in Fig. 1C.

To evaluate the suitability of antibody-functionalised NPs for the detection of complex bio-active molecules, anti-EPO functionalised NPs were allowed to interact with the human urinary EPO international standard (HuEPO IS) and then screened by Raman spectroscopy. The antibody-functionalised NPs were compared

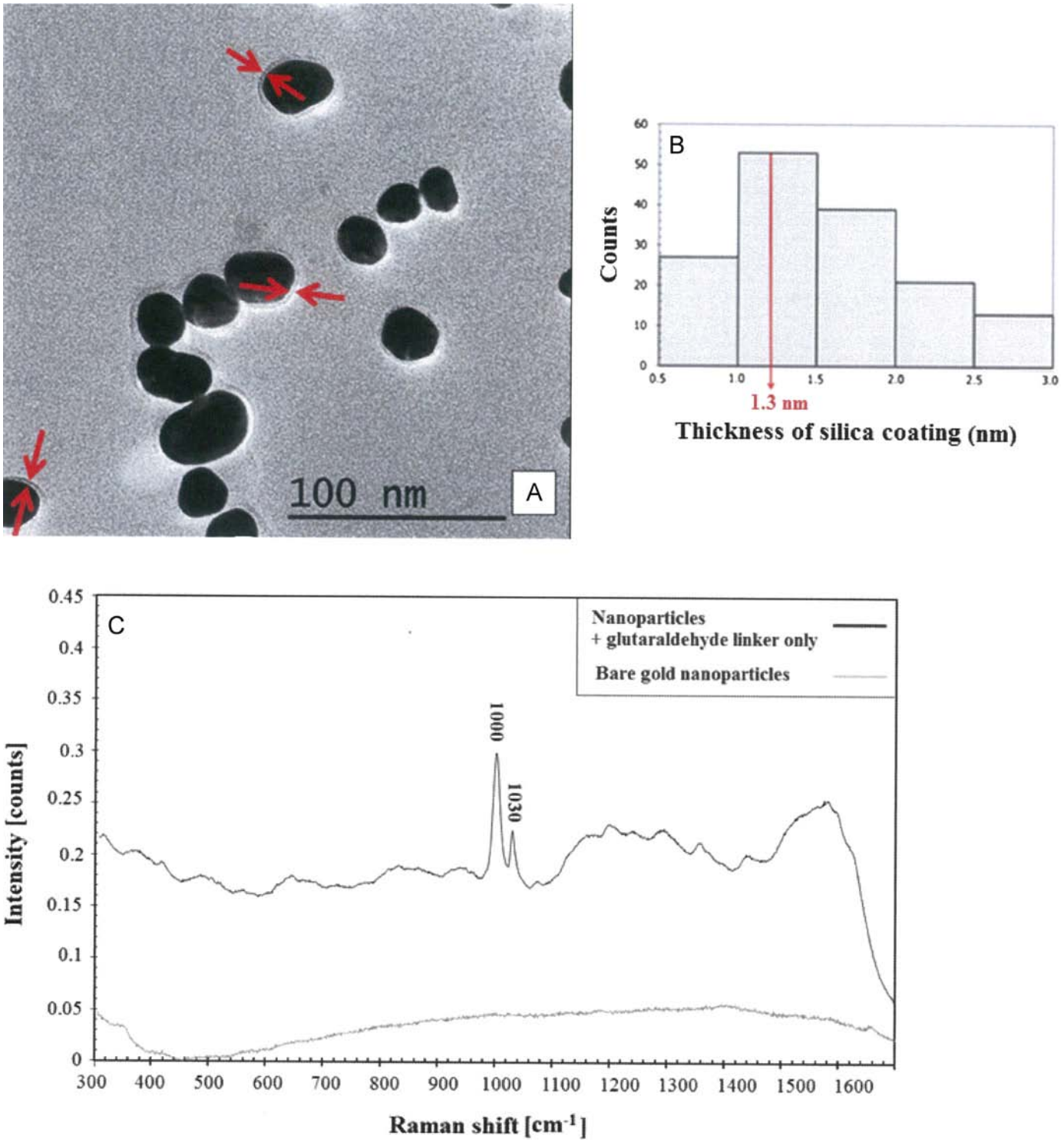

Fig. 1. (A) TEM of the silica-coated nanoparticles (the silica shell is indicated by the arrows). (B) The range and median thickness of the silica shell, $n=153$. (C) The Raman spectra of the gold nanoparticles before and after attachment of glutaraldehyde linker.

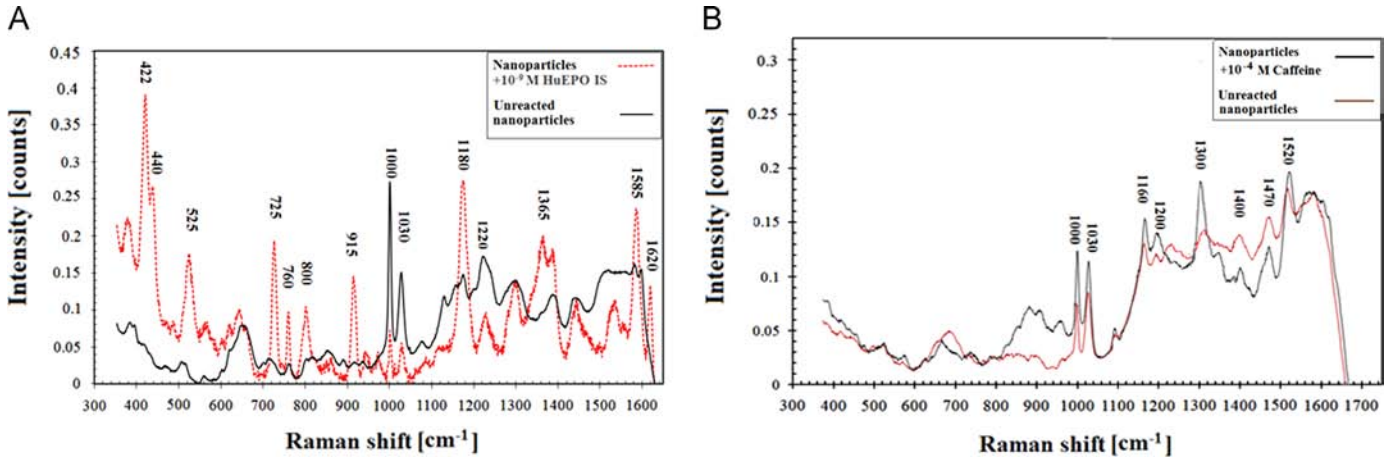

Fig. 2. (A) Raman spectra of nanoparticles functionalised with anti-EPO antibody before and after interaction with 1×10^{-9} M HuEPO international standard. (B) Raman spectra of nanoparticles functionalised with anti-caffeine antibody before and after interaction with 1×10^{-4} M caffeine standard.

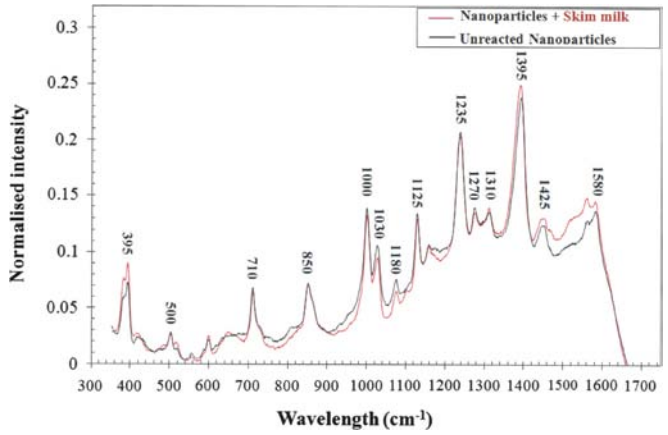

Fig. 3. Average spectra of 12 replica measurements for EPO antibody-functionalised nanoparticles before and after interaction with skim milk.

before and after their interaction with HuEPO (Fig. 2A). The emergence of new bands at 422 cm^{-1}, 725 cm^{-1}, 800 cm^{-1}, 915 cm^{-1} and the shift of the bands at 525 cm^{-1}, 1365 cm^{-1}, 1585 cm^{-1}, 1620 cm^{-1} from their original positions in the spectrum of the un-reacted species are attributable in part to antibody conformational rearrangements upon binding EPO to the antibody fragment antigen binding (Fab) regions [13]. The band intensities are consistent with a strong binding interaction between the analyte and the antibody that immobilized EPO molecules close to the NP surface, allowing the observed enhancement in the Raman spectrum [4,6,13].

The significant bands observed at 1000 cm^{-1} and 1030 cm^{-1} are characteristic of pyridine ring vibrational modes [22] and arise as a result of our method of cross-linking the antibody to the modified silica surface. The glutaraldehyde linker attachment to the modified silica surface involves the reaction between glutaraldehyde and the terminal amine groups of the silica shell. The reaction of glutaraldehyde with amines has been reported to result in some dimerization [23,24], such as the formation of quaternary pyridinium compounds [25]. The formation of the pyridinium species would give rise to pyridine bands in the SERS spectra of the antibody-functionalized NPs.

The suitability of the proposed nanosensor strategy for the direct detection of simple bioactive molecules was evaluated using NPs functionalized with an anti-caffeine antibody for the SERS detection of caffeine. The SERS spectrum of the NPs before and after interaction with caffeine characteristically showed a significantly enhanced band intensity at 1300 cm^{-1} (Fig. 2B), which can be attributed to the stretching vibration mode of the imidazole ring in the caffeine molecule [26,27].

The 1.3 nm silica shell not only enabled the direct detection of the target analyte by allowing the antibody and analyte to reside within the LSPR field, but likely also improved the SERS enhancement at the Raman hot spots. Tian et al., have shown that a 1 nm thick silica shell Au@SiO_2 NPs produced about twice the enhancement of comparable bare Au NPs. The added enhancement was attributed, in part, to the formation of hot spots at the silica shell inserts between the NPs [28].

To confirm the selectivity of the antibody-functionalised NPs and to investigate their cross-reactivity with potentially interfering analytes in protein-rich biological fluids, skim milk was allowed to react with NPs functionalised with EPO antibody. No significant change in the spectrum of the unreacted NPs was observed after their interaction with skim milk (Fig. 3), confirming that the EPO antibody did not cross-react with the proteins found in skim milk. It further showed that the passive silica shell also prevented the milk proteins from binding directly to the surface of the NPs and contributing extraneous features to the Raman spectrum. The variation in signal intensities within the Raman spectra of the unreacted nanoparticles (Figs 2–4) may be attributed in part to the inconsistent number of active antibody attachments on the surface of the nanoparticles.

To confirm that the ethylamine blocking agent adequately blocked any unreacted glutaraldehyde linker sites on the antibody-functionalised NPs, diet Coke™ was reacted with anti-caffeine antibody functionalised NPs. Diet Coke™ contains the organic sweetener aspartame, which is a methyl ester of the L-aspartic acid and L-phenylalanine dipeptide [29]. Aspartame contains a primary amine moiety that can potentially react with unreacted glutaraldehyde cross linker on the NP. A comparison of the Raman spectrum of the antibody-functionalised nanoparticles after the addition of diet coke with the Raman spectrum of the unreacted NPs revealed no significant differences (Fig. 4). This confirmed that there were no unblocked linker sites available to cross-react with the amine groups of the organic sweetener.

To determine the sensitivity of the nanosensors towards their respective bio-active analyte, two series of diluted aqueous solutions, one of rHuEPO IS and one of caffeine, were prepared and interacted with the relevant antibody-functionalised NPs. The intensities of the characteristic SERS bands at 422 cm^{-1} (for rHuEPO) and 1300 cm^{-1} (for caffeine) were monitored to follow the interaction between the functionalised NP and the analytes at various concentrations. The peak intensities at the 422 cm^{-1} and

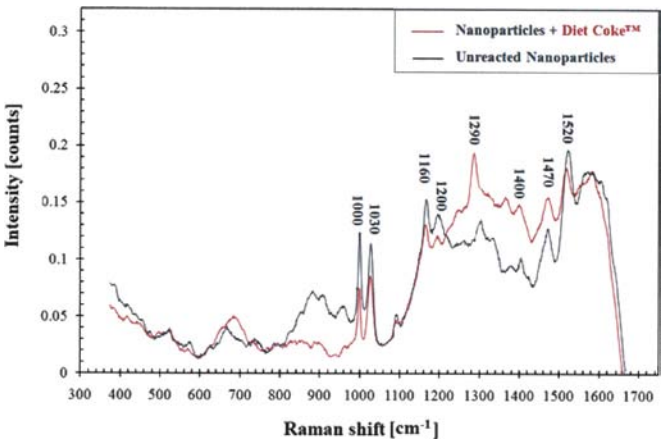

Fig. 4. Average spectra of 6 replica measurements for caffeine antibody-functionalised nanoparticles before and after their interaction with caffeine-free Diet Coke™.

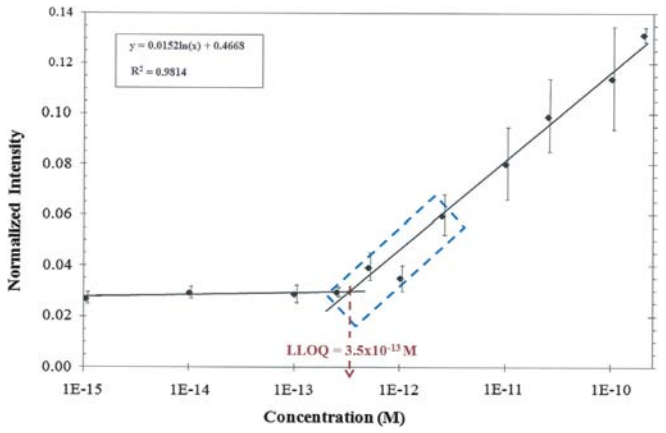

Fig. 5. Linear calibration curve of rHuEPO (at 422 cm^{-1}) in the concentration range 2×10^{-10} M to 1×10^{-15} M (LLOQ=3.5×10^{-13} M). The dotted region encompasses the normal concentration range of EPO in biological fluids.

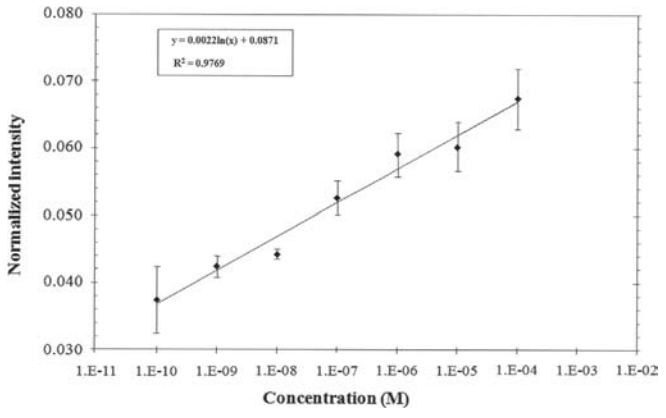

Fig. 6. Linear calibration curve of caffeine (at 1300 cm^{-1}) in the concentration range of 1×10^{-4} M to 1×10^{-10} M (LLOQ=1×10^{-10} M).

1300 cm^{-1} are assigned to the CH_2 vibration mode of the acyl chains in EPO [30,31,32] and the Imidazole trigonal ring stretching of caffeine [33,34], respectively. The relationship between the normalised peak intensity and the log concentration of rHuEPO is shown in Fig. 5. The R^2 value of the linear relationship in the concentration range of 10^{-10} M to 3.5×10^{-13} M was 0.9814 indicating the accuracy of the quantification. The lower limit of quantification (LLOQ) for EPO was found to be 3.5×10^{-13} M, which is comparable to the concentrations of EPO in human urine [35]. Therefore the EPO antibody-functionalised NPs are suitable for practical applications like the rapid SERS detection of EPO abuse in biological fluids from athletes prior to major sporting events. The calibration curve for caffeine at 1300 cm^{-1} was log linear over five orders of magnitude, to a LLOQ of 1×10^{-10} M (Fig. 6). The R^2 value of the calibration curve was 0.9769 indicating the accuracy of the quantification. As the lowest concentration of caffeine found in commercial caffeinated beverages is approximately 1×10^{-6} M (decaffeinated coffee) [36], the anti-caffeine antibody functionalised NP is similarly suitable for analysis of caffeine-containing beverages.

The drop-dry technique was used for the quantitative analysis of EPO and caffeine as it improves the SERS applicability and sensitivity in comparison to measurements directly from NP colloidal solution [37]. In this technique, 10 μL of the analyte standard solution is mixed with an equal volume of the functionalized gold nanoparticles. The sample was then deposited on a microscope slide and left to completely air-dry to form a ring in the edge part of the drop. The evaporation of the solvent allows almost the nanoparticles to aggregate and, in effect, form hot spots. The development of high density hot spots inside the ring leads to enormous SERS enhancement. The drop-dry technique also guarantees that the total mass of the analyte (EPO or caffeine) is quantitatively deposited onto the surface of the functionalised nanoparticles clusters. The formed ring is then screened at multiple spots in order to acquire an average Raman spectrum that is a true representative of the entire dried sample. These procedures are maintained to all samples to guarantee the reliability of the quantification and LLOQ of the analyte.

4. Conclusion

Here we have described a rapid and sensitive analytical technique that is applicable for the direct detection of ultra trace amounts of both large and small bio-active molecules. This method utilizes label-free SERS to quantitatively detect EPO and caffeine through their molecular fingerprint and/or the altered fingerprint of their respective antibody upon binding. The observed lack of cross-reactivity suggests that this nannosensor design is suitable for detecting analytes directly in their relevant context (i.e. biological fluids or beverage products). With the current technological advancements in Raman spectrometers, our nanosensors have the potential for the field detection of ultra-trace amounts bio-active compounds. For example, when combined with a portable Raman spectrometry platform, the two nanosensors described here can be adapted to rapidly screen either EPO- or caffeine-containing samples on site within the food, clinical diagnosis and sports industries.

Acknowledgements

The authors are grateful for the funding support from the Partnership for Clean Competition (PCC) research scheme (USA), grant number (RM2013000476).

References

[1] E.C. Le Ru, M. Meyer, P.G. Etchegoin, J. Phys. Chem. B 110 (2006) 1944–1948.
[2] A.M. Michaels, M. Nirmal, L.E. Brus, J. Am. Chem. Soc. 121 (1999) 9932–9939.
[3] M. Moskovits, J. Raman Spectrosc. 36 (2005) 485–496.
[4] R. Kast, S. Tucker, K. Killian, M. Trexler, K. Honn, G. Auner, Cancer Metastasis Rev. (2014) 1–21, http://dx.doi.org/10.1007/s10555-013-9489-6.
[5] D.L. Jeanmaire, R.P. Van Duyne, J. Electroanal. Chem. Interfacial Electrochem 84 (1977) 1–20.
[6] K. Kneipp, H. Kneipp, J. Kneipp, Acc. Chem. Res. 39 (2006) 443–450.
[7] X.X. Han, B. Zhao, Y. Ozaki, Anal. Bioanal. Chem. 394 (2009) 1719–1727.

[8] P. Etchegoin, H. Liem, R.C. Maher, L.F. Cohen, R.J.C. Brown, M.J.T. Milton, J.C. Gallop, Chem. Phys. Lett. 367 (2003) 223–229.
[9] X.X. Han, H.Y. Jia, Y.F. Wang, Z.C. Lu, C.X. Wang, W.Q. Xu, B. Zhao, Y. Ozaki, Anal. Chem. 80 (2008) 2799–2804.
[10] J. Kneipp, H. Kneipp, K. Kneipp, Chem. Soc. Rev. 37 (2008) 1052–1060.
[11] L. Xu, C. Zong, X. Zheng, P. Hu, J. Feng, B. Ren, Anal. Chem. 86 (2014) 2238–2245.
[12] X.X. Han, L. Chen, W. Ji, Y. Xie, B. Zhao, Y. Ozaki, Small 7 (2011) 316–320.
[13] S.P. Mulvaney, M.D. Musick, C.D. Keating, M.J. Natan, Langmuir 19 (2003) 4784–4790.
[14] M. Sanles-Sobrido, L. Rodriguez-Lorenzo, S. Lorenzo-Abalde, A. Gonzalez-Fernandez, M.A. Correa-Duarte, R.A. Alvarez-Puebla, L.M. Liz-Marzan, Nanoscale 1 (2009) 153–158.
[15] X.X. Han, Y. Kitahama, Y. Tanaka, J. Guo, W.Q. Xu, B. Zhao, Y. Ozaki, Anal. Chem. 80 (2008) 6567–6572.
[16] C. Andreou, M.R. Hoonejani, M.R. Barmi, M. Moskovits, C.D. Meinhart, ACS Nano 7 (2013) 7157–7164.
[17] I. Freitag, U. Neugebauer, A. Csaki, W. Fritzsche, C. Krafft, J. Popp, Vib. Spectrosc. 60 (2012) 79–84.
[18] X.X. Han, L.J. Cai, J. Guo, C.X. Wang, W.D. Ruan, W.Y. Han, W.Q. Xu, B. Zhao, Y. Ozaki, Anal. Chem. 80 (2008) 3020–3024.
[19] K.K. Maiti, U.S. Dinish, C.Y. Fu, J.-J. Lee, K.-S. Soh, S.-W. Yun, R. Bhuvaneswari, M. Olivo, Y.-T. Chang, Biosens. Bioelectron. 26 (2010) 398–403.
[20] H. Xia, S. Bai, J.r. Hartmann, D. Wang, Langmuir 26 (2009) 3585–3589.
[21] J.F. Li, S.-B. Li, J.R. Anema, Z.-L. Yang, Y.-F. Huang, Y. Ding, Y.-F. Wu, X.-S. Zhou, D.-Y. Wu, B. Ren, Z.-L. Wang, Z.-Q. Tian, Appl. Spectrosc. 65 (2011) 620–626.
[22] M. Muniz-Miranda, G. Cardini, V. Schettino, Theor. Chem. Acc. 111 (2004) 264–269.
[23] P.M. Hardy, A.C. Nicholls, H.N. Rydon, J. Chem. Soc., Perkin Trans 1 (1976) 958–962.
[24] P.M. Hardy, G.J. Hughes, H.N. Rydon, J. Chem. Soc., Perkin Trans 1 (1979) 2282–2288.
[25] I. Migneault, C. Dartiguenave, M.J. Bertrand, K.C. Waldron, BioTechniques 37 (2004) 790–802.
[26] H.G.M. Edwards, T. Munshi, M. Anstis, Spectrochim. Acta, Part A 61 (2005) 1453–1459.
[27] I. Pavel, A. Szeghalmi, D. Moigno, S. Cîntă, W. Kiefer, Biopolymers 72 (2003) 25–37.
[28] X.D. Tian, B.J. Liu, J.F. Li, Z.L. Yang, B. Ren, Z.Q. Tian, J. Raman Spectrosc. 44 (2013) 994–998.
[29] B.A. Magnuson, G.A. Burdock, J. Doull, R.M. Kroes, Crit. Rev. Toxicol. 37 (2007) 629–727.
[30] J.J. Duindam, G.F. Vrensen, C. Otto, J. Greve, IOVS 39 (1998) 94–103.
[31] J.A. Brailsford, S.J. Danishefsky, PNAS 109 (2012) 7196–7201.
[32] H.F. Bunn, Blood 99 (2002) 1503–1504.
[33] J. Kang, H. Gu, L. Zhong, Y. Hu, F. Liu, Spectrochim. Acta, Part A 78 (2011) 757–762.
[34] H.G.M. Edwards, T. Munshi, M. Anstis, Spectrochim. Acta, Part A 61 (2005) 1453–1459.
[35] M. Lonnberg, M. Drevin, J. Carlsson, J. Immunol. Methods 339 (2008) 236–244.
[36] C. Haskell, D. Kennedy, A. Milne, K. Wesnes, Appetite 50 (2008) 559.
[37] P. Šimáková, M. Procházka, E. Kočišov, Spectrosc. Int. J. 27 (2012) 449–453.